Vietnam Journal of Earth Sciences, 47(2), 151-175, https://doi.org/10.15625/2615-9783/22192

Vietnam Journal of Earth Sciences
https://vjs.ac.vn/index.php/jse

Forest cover change mapping based on Deep Neuron Network, GIS, and High-resolution Imagery

Nguyen Thanh Hoan[1], Ho Le Thu[1], Nguyen Van Dung[1], Hoa Thuy Quynh[1], Nguyen Kim Anh[1], Le Duc Hanh[1], Pham Van Duan[4], Phan Trong Trinh[2], Tran Van Phong[2,3*]

[1]*Institute of Geography, Vietnam Academy of Science and Technology, Hanoi, Vietnam*
[2]*Institute of Geological Sciences, Vietnam Academy of Science and Technology, Hanoi, Vietnam*
[3]*Graduate University of Science and Technology, Vietnam Academy of Science and Technology, Hanoi, Vietnam*
[4]*Institute for Forest Ecology and Environment, Vietnam National University of Forestry, Hanoi, Vietnam*

Received 19 September 2024; Received in revised form 15 October 2024; Accepted 08 January 2025

ABSTRACT

With the rapid advancement of technology, monitoring forest cover changes has become increasingly quantifiable through various techniques and methods. In this study, we developed a procedure that utilizes the Deep Neuron Network (DNN) model and the Geographic Information Systems (GIS) based on high-resolution imagery captured at different time points to create forest cover change maps in Nui Luot, Chuong My, Hanoi. Two RGB (Red-Green-Blue) spectral images were captured by Unmanned Aerial Vehicle (UAV) at two different time points (pre-scene and post-scene) and used to extract information for the DNN model to produce land cover maps for these two time points. The land cover classification was divided into four classes: (1) Trees, (2) Vacant, (3) Built area and others, and (4) Water surface. Combined with GIS analysis, the forest cover change maps were developed to quantify detailed increases or losses in forest cover based on the "Trees" class. The model's accuracy was evaluated using parameters such as the area Under the ROC Curve (AUC), Accuracy (ACC), Precision, Recall, F1-Score, Kappa, and Root Mean Square Error (RMSE). The analysis results indicate that from January 31, 2023, to October 20, 2023, the forest cover in the study area decreased by 0.53%. The accuracy metrics for the pre-change scene were: average AUC = 0.922, ACC = 76.86%, average Precision = 0.743, average Recall = 0.73, average F1-Score = 0.723, Kappa = 0.692, and RMSE = 0.297. For the post-change scene, the accuracy metrics were: average AUC = 0.954, ACC = 81.89%, average Precision = 0.823, average Recall = 0.815, average F1-Score = 0.818, Kappa = 0.758, and RMSE = 0.262. A deforestation scenario was constructed to evaluate the effectiveness of the DNN models in assessing and monitoring forest dynamics.

Keywords: Deep Learning, UAV, forest cover change, Nui Luot, land cover.

1. Introduction

On a global scale, forest cover is continuing to decline due to the impacts of climate change and human activities (Diez et al., 2021; UN, 2024; Weisse, Goldman and Carter, 2024). According to statistics, in 2023 alone, 3.75 million hectares of primary forest were lost (Weisse, Goldman and Carter, 2024). Among the areas most severely affected are the tropical forests of the Amazon

*Corresponding author, Email: tphong1617@gmail.com

(Brazil), the Democratic Republic of the Congo (DRC), and Indonesia (Weisse, Goldman and Carter, 2024), with Vietnam also being one of the countries impacted by the gradual loss of forest cover (Cochard et al., 2016). One of the solutions to manage and mitigate deforestation is the application of technologies in forest monitoring (Henry et al., 2015). Remote sensing tools, satellite imagery, Unmanned Aerial Vehicle (UAV) imagery, and artificial intelligence (AI) are being widely utilized for real-time monitoring of forest dynamics, facilitating early detection of illegal logging activities (Buchelt et al., 2024; Dainelli et al., 2021; Ecke et al., 2022; Giang Linh, Dang Kinh and Bui Thanh, 2023; Guimarães et al., 2020; Liu et al., 2021; Pham-Duc, Tran Anh and Tong Si, 2023; Tran Xuan et al., 2023). Forest change maps serve as valuable tools in forest monitoring technology to track and analyze changes in forest area and quality over time (Hansen and Loveland, 2012; Kim et al., 2014). These maps are typically used for (1) Monitoring forest loss and recovery by providing information on deforestation due to logging, agriculture, or other causes, as well as the recovery of areas that have been devastated (Camarretta et al., 2020). (2) Assessing the impacts of climate change to understand better how climate change affects forest ecosystems, including changes in species distribution and forest structure (Yang et al., 2019). (3) Management and conservation to assist forest managers in planning conservation efforts and sustainable management strategies while also identifying areas that require priority protection (Camarretta et al., 2020; Yang et al., 2019). (4) Ecological research by providing data for studies on biodiversity, soil nutrition, and other ecological factors (Hill et al., 2019; Marín et al., 2021).

AI, particularly machine learning and deep learning methods, has opened up new potentials in classifying and predicting changes in forest cover (Diez et al., 2021; Janga et al., 2023; Khan et al., 2017; Khelifi and Mignotte, 2020; Ortega et al., 2019). AI algorithms can learn from historical data and make more accurate predictions about forest cover changes based on various input factors such as remote sensing data, topography, climate, and human activities (Diez et al., 2021; Isaienkov et al., 2021; Janga et al., 2023; Khelifi and Mignotte, 2020; LeCun, Bengio and Hinton, 2015). The application of AI, remote sensing, and GIS in forest cover mapping not only aids in monitoring changes over time but also plays a crucial role in providing early warnings about deforestation (Annus et al., 2021; Watanabe et al., 2021), environmental degradation, and supports policymakers in sustainable forest resource management (Haq et al., 2024; Lechner, Foody and Boyd, 2020). These advanced technologies have contributed to global efforts in forest protection, biodiversity conservation, and mitigating the impacts of climate change (Haq et al., 2024; Janga et al., 2023).

In recent years, research on forest cover changes using imagery from UAV combined with advanced AI tools has become a prominent trend in the fields of remote sensing and environmental monitoring (Diez et al., 2021; Ecke et al., 2022; Mohan et al., 2021). UAV provide high-resolution spatial data and flexibility, allowing detailed information to be collected in hard-to-reach areas (Chenyan et al., 2024; Diez et al., 2021; Ecke et al., 2022; Grubesic, Nelson and Wei, 2024; Guimarães et al., 2020; Mohan et al., 2021). UAV equipped with optical cameras, particularly RGB spectral channels, are widely used due to their cost-effectiveness

and simple data structure (Bourgoin et al., 2020; Diez et al., 2021; Li et al., 2020; Schiefer et al., 2020). Successful applications of deep learning combined with UAV RGB imagery analysis in forest change studies include research by Onishi and Ise (2021), who utilized Convolutional Neural Networks (CNN) to successfully classify seven tree classes with over 90% accuracy at the Kamigamo Experimental Station of Kyoto University (Onishi and Ise, 2021). A similar study employing CNN to analyze high-resolution UAV RGB imagery (Schiefer et al., 2020) accurately mapped nine tree species, three genus-level classes, dead wood, and forest floor with an F1-score accuracy of 0.73 in temperate forest areas of the Southern Black Forest and Hainich National Park in Germany (Schiefer et al., 2020). Xie et al. (2024) used the Mask R-CNN model to create high-accuracy forest maps based on high-resolution UAV RGB images in Jiangle County, Fujian Province, China (Xie et al., 2024). These examples demonstrate the significant potential of applying deep learning models combined with high-resolution UAV RGB imagery analysis for forest cover change identification and mapping.

The DNN serves as a foundational model for deep learning techniques, offering several advantages such as (1) the ability to learn complex features: DNN have multiple hidden layers, allowing them to learn intricate and nonlinear features from data (Aldahdooh et al., 2022; Hussain, Tamizharasan and Rahul, 2022). This makes them suitable for tasks such as image recognition, speech recognition, and natural language processing (Hussain, Tamizharasan, and Rahul, 2022); (2) automatic feature extraction: One of the most significant advantages of DNN is their ability to automatically extract essential features from raw data without human intervention, minimizing reliance on manual feature selection techniques (Du et al., 2018); (3) high performance with large datasets: DNN often outperforms traditional methods when large amounts of data are available for training (Faker and Dogdu, 2019; Rithani, Kumar and Doss, 2023). It can leverage information from large datasets to enhance the accuracy and generalization capabilities of the model (Faker and Dogdu, 2019; Rithani, Kumar and Doss, 2023); and (4) scalability: DNN are flexible and can scale with various data types, from structured data to unstructured data such as images, audio, and text (Aldahdooh et al., 2022; Du et al., 2018; Hussain, Tamizharasan and Rahul, 2022).

With the advantages of DNN models and high-resolution UAV RGB imagery outlined above, this study presents a procedure for applying a DNN model based on high-resolution UAV RGB image analysis and GIS techniques to create forest cover change maps over two different periods. The experimental study area is the Luot Mountain area in Chuong My, Hanoi, with forest cover dynamics analyzed using two optical RGB images captured at different times (pre-scene: January 1, 2023, and post-scene: October 20, 2023). Accordingly, two land cover classification maps were created with four classes (Trees, vacant, built area, and others, as well as water surface). The 'Trees' class was extracted using GIS analysis to develop the forest cover change map for the study area. The results of this research contribute to assisting managers in the planning and rational use of forest land and demonstrate the potential applications for high-accuracy forestry research.

2. Research area

The study area is part of Luot Mountain, covering an area of 209.3 hectares, located in the center of Xuan Mai Town, 38 km from the center of Hanoi, and 45 km from Hoa Binh Town (Fig. 1). Luot Mountain features relatively uniform terrain characterized by low hills, with minimal fragmentation, comprising two contiguous hills extending approximately 2 km from east to west. One peak has an absolute height of 133 m, while the other reaches 76 m, with an average slope of 15 degrees and a maximum slope of 27 degrees. The primary aspects are northeast, northwest, and southeast. The terrain conditions are favorable for afforestation. Several indigenous tree species, such as Diospyros spp, Hopea odorata, and Dalbergia tonkinensis, have been planted in this area. The soil in the Luot Mountain area is yellow-brown Feralit soil developed on the parent rock of Porphyry belonging to the neutral magma rock group, with thickness varying from thick to medium depending on the specific topographical location.

Climate: Luot Mountain is situated within the humid tropical monsoon climate zone, characterized by two distinct seasons: the rainy season from April to October and the dry season from November to March of the following year.

- Temperature Regime: The average annual temperature is 23.2°C, with the highest average monthly temperatures in July and August reaching 28.5°C and the lowest average in January at 16.5°C. The hot season sees temperatures exceeding 25°C from May to mid-September, while the cold season has average temperatures below 20°C from December to March of the following year. The remaining months have average temperatures ranging from 20 to 25°C.

- Precipitation Regime: The total annual rainfall is 1753 mm, with an average monthly rainfall of 146 mm. Rainfall is unevenly distributed throughout the year, with the highest average monthly rainfall occurring in July and August at 312 mm and the lowest in January at 15 mm.

- Humidity: The average relative humidity is relatively high at 84% but varies significantly between months.

- Evaporation: The average annual evaporation is 602 mm, with the highest in May (78.5 mm) and the lowest in February (47.6 mm).

- Wind Regime: The area is influenced by two main wind directions:

o The Southeast monsoon blows from April to October.

o The Northeast monsoon blew from November to March of the following year.

The area is traversed by two rivers, surrounded by the Bui and Tich rivers, with a total river and stream area of 29.43 hectares. Additionally, there are water reservoirs and dam systems, such as Vai Bon Lake and the Tran Dam.

Flora Resources: The experimental forest at Luot Mountain has recorded 342 species of vascular plants belonging to 257 genera and 90 families. The vegetation in the area is diverse in life forms and values, comprising 9 life forms and 7 value groups.

Fauna Resources: The area has recorded 156 species of vertebrates from 20 orders, 60 families, and 104 genera, including 21 rare species. Furthermore, 409 insect species have been identified from 87 families and 13 orders, with the order Lepidoptera accounting for 208 species, 135 genera, 30 families, 10 classes, and 4 species.

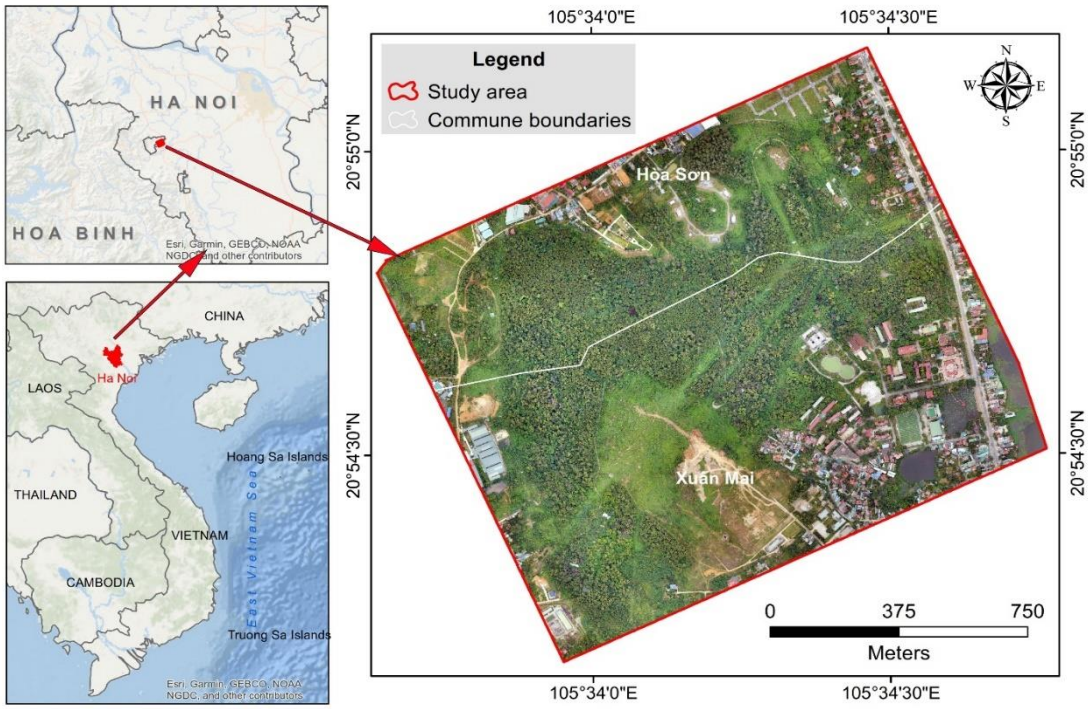

Figure 1. Study area in a part of Luot mountain, Chuong My, Hanoi

3. Methodology and data used

3.1. Methodology

The research methods and techniques employed are illustrated in an 8-step process (Fig. 2). The sequence of steps is as follows:

Step 1: Select the study area at Luot Mountain (Fig. 1).

Step 2: Collect the database: Gather UAV imagery with RGB spectral channels at two different time points (Fig. 2). Details about the collected data are presented in the data section.

Step 3: Sample data for the model: Samples are determined based on location through analysis of the imagery and verified through fieldwork. Thus, the input data for the model includes 3 RGB bands. The label data comprises 4 classes: (1) Trees, (2) Vacant, (3) Built area and others, and (4) Water surface. These sample data are organized into two approaches: Option 1 separates training and validation datasets for each imagery scene. Option 2 combines the training data of the pre-scene and post-scene into a single training dataset while maintaining the validation datasets for each imagery scene.

Step 4: Model implementation using a DNN model applied through the WekaDeeplearning4j tool in Weka software version 3.8.6 (Lang et al., 2019). This tool features an intuitive and user-friendly graphical user interface (GUI) that is easy to use.

Step 5: Evaluate the model results using assessment parameters for multi-class classification problems, such as ROC, AUC-ROC, Accuracy, Precision, F1-Score, Recall, Kappa, and RMSE.

Step 6: Select the optimal option based on the model evaluation results from Step 5. In this study, Option 1 was chosen to facilitate the creation of the land cover map. An additional scenario to verify the model's accuracy assumes areas of lost forest cover in the post-scene imagery (Fig. 3). Accordingly,

these areas in the post-scene are color-coded in gray, and a land cover map based on this scenario is established.

Step 7: Create the land cover map based on the DNN model from the pre- and post-scene. A land cover map verifies the model after classification is created according to the deforestation scenario.

Step 8: Use GIS technology to analyze and develop a forest cover change map. The tool utilized is ArcMap 10.8 [ESRI Inc].

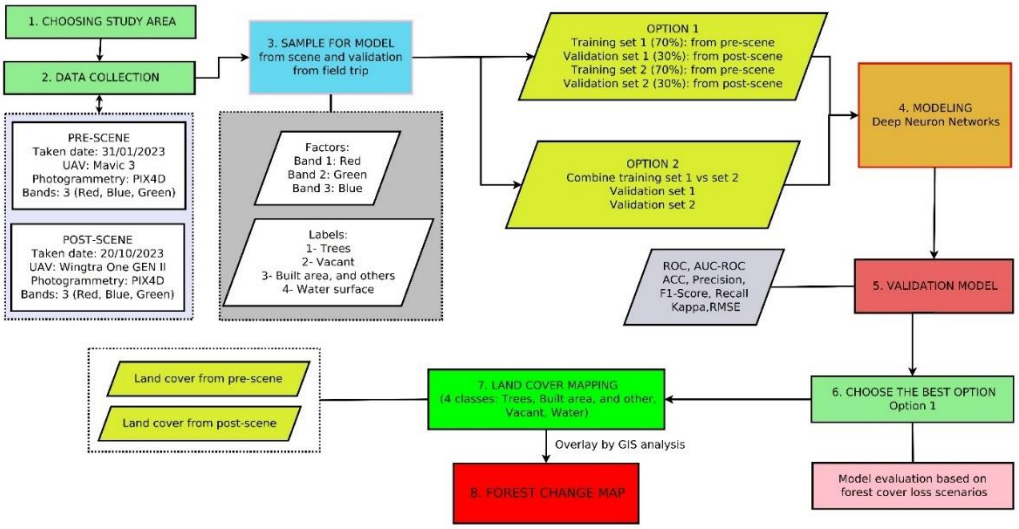

Figure 2. Flow chart processing in this study

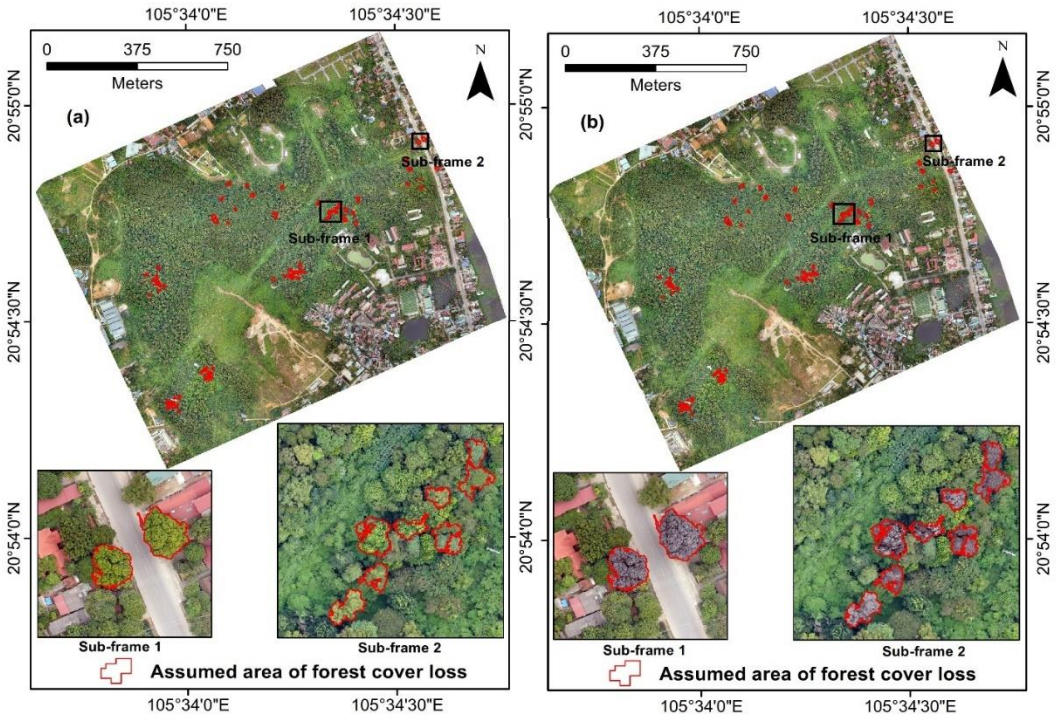

Figure 3. Delineation of areas for the hypothetical deforestation scenario: (a) post-scene, (b) the scene after revision according to the deforestation script of the post-scene

3.1.1. Generating photogrammetry imagery from UAV images

The basic steps to create maps from UAV imagery include:

(1) Data Collection: Fly the UAV over the area of interest and collect aerial images with an inevitable overlap between them.

(2) Data Preprocessing: Perform basic edits on the images, such as color balancing, noise reduction, and brightness adjustment.

(3) Image Stitching: Use PIX4D software to stitch the images into a sizeable ortho mosaic image (Caputo et al., 2023). The software employs algorithms to identify common points between the images and merge them (Caputo et al., 2023).

(4) Georeferencing: Assign spatial coordinates to the stitched image to create a map that can be utilized in GIS.

3.1.2. Deep Neuron Network model

DNN is characterized by a structure that includes multiple layers, particularly hidden ones (Liu et al., 2017; Shrestha and Mahmood, 2019). These networks are widely used in AI and machine learning to model complex relationships in data (Liu et al., 2017). The operation of DNN relies on neurons and their connections (LeCun, Bengio, and Hinton, 2015). Each neuron in a layer receives input from the neurons of the previous layer, computes the output, and transmits the result to the next layer (Shrestha and Mahmood, 2019). The network learns to adjust weights through a training process using the backpropagation algorithm and optimizes them using algorithms like gradient descent (Shrestha and Mahmood, 2019). DNN is notable for its ability to automatically learn features from complex and nonlinear data, which traditional models struggle to handle (Samek et al., 2017). DNN form the foundation of deep learning algorithms, enabling them to tackle various tasks ranging from computer vision to natural language processing (Liu et al., 2017). Figure 4 illustrates how the DNN model classifies land cover from UAV RGB images. Table 1 presents the hyperparameters of the DNN model used in this study.

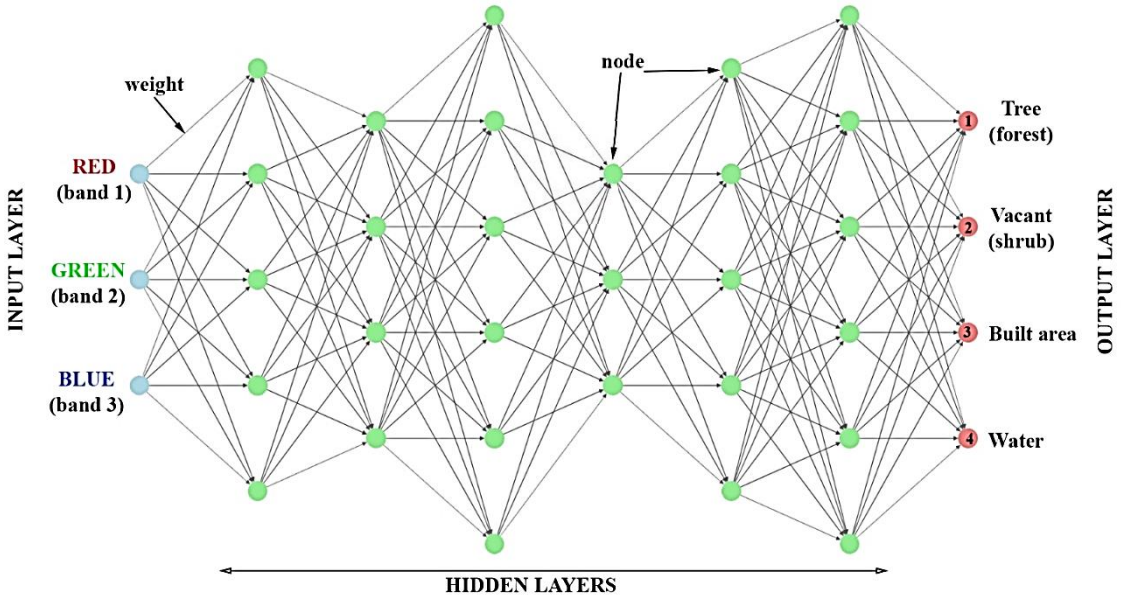

Figure 4. Illustration of the multilayer neural network of Deep Learning for classifying forest cover from high-resolution UAV imagery in the Luot Mountain area

Table 1. The hyperparameters of the DNN model

Hyperparameters	Feature/Value
Layer specification	
Input layer	3 node
Number of hidden layers	6
Number of nodes in hidden layers	29
Output layer	4 node
Connection	full
Activation	Softmax
Loss function	MCXENT
Number of epochs	10
Batch size	100
Network configuration	
Optimization algorithm	Stochastic gradient descent
Updater	Adam
Bias Updater	Sgd
Learning rate	0.001
Weight initialization method	XAVIER
Bias initialization	0.0

Basic Structure of DNN

Input Layer: Receives input data and passes it to the hidden layers. Each neuron in the input layer corresponds to a feature of the data.

- Hidden Layers: These layers lie between the input and output layers, where complex computations occur. Each hidden layer consists of multiple neurons, allowing the network to learn more abstract and complex features.

- Output Layer: Provides the network's final results. Depending on the type of problem, the output layer may represent probabilities for classification classes or continuous values for regression tasks.

Activation Functions

Activation functions are crucial components in DNN that help the network learn the nonlinear characteristics of the data:

- ReLU (Rectified Linear Unit): Commonly used in hidden layers, the formula ReLU facilitates faster learning and mitigates the vanishing gradient problem.

- Sigmoid: Maps input values to a range between 0 and 1, typically used for binary classification.

- Tanh: Converts input values to a range between -1 and 1, enabling faster and more stable learning than Sigmoid.

- Softmax: Converts outputs into probabilities for multi-class classification.

Training Process

- Forward Propagation: The process of passing data through the network's layers to compute the output.

- Loss Function: Measures the difference between the network's predictions and the actual values. For example, MSE (Mean Squared Error) is used for regression, and Cross-Entropy is used for classification.

- Backpropagation: Computes the gradient of the loss function to the network's weights and updates the weights using optimization algorithms.

Optimization Algorithms

- Gradient Descent: Adjusts weights in the direction of the negative gradient of the loss function to minimize loss.

- Adam (Adaptive Moment Estimation): A more efficient optimization algorithm that adjusts the learning rate based on the first and second moments of the gradient.

Regularization

Techniques to prevent overfitting and improve the network's generalization ability:

- Dropout: Randomly removes some neurons during training to prevent the network from relying too heavily on certain neurons.

- L2 Regularization: Adds a penalty to the loss function based on the sum of the squares of the weights, helping to reduce model complexity.

3.1.3. Methods for evaluating model accuracy

To evaluate the accuracy of the DNN model in the land cover classification task, the evaluation metrics used in this study include the Confusion Matrix, Area Under the Curve (AUC), Accuracy, Precision, Recall, F1-Score, Kappa, and RMSE (Maxwell et al., 2017; Rodriguez-Galiano and Chica-Rivas, 2014).

Confusion Matrix

The Confusion Matrix is a machine learning tool used to assess a classification

model's performance. This matrix displays the number of predictions made by the model for each class, allowing for a comparison between the predictions and the actual values (Marom, Rokach, and Shmilovici, 2010). The structure of a 4-class confusion matrix C for the land cover classification problem in this study is as follows:

$$C = \begin{bmatrix} C_{11} & C_{12} & C_{13} & C_{14} \\ C_{21} & C_{22} & C_{23} & C_{24} \\ C_{31} & C_{32} & C_{33} & C_{34} \\ C_{41} & C_{42} & C_{43} & C_{44} \end{bmatrix} \quad (1)$$

where: C_{ii} (với i = 1, 2, 3, 4) is the number of correct predictions for each corresponding class (Vacant; Water; Built area and others; Trees). C_{ij} ($i \neq j$) is the number of incorrect predictions, meaning samples belonging to class i but incorrectly predicted as class j.

Accuracy (ACC)

The accuracy parameter is a commonly used measure to evaluate the performance of classification models in machine learning and artificial intelligence. It measures the ratio of correct predictions to the total number of predictions. Accuracy indicates the percentage of data samples the model can correctly classify (Rodriguez-Galiano and Chica-Rivas, 2014). The formula for calculating accuracy is as follows:

$$\text{Accuracy} = \frac{\sum_{i=1}^{4} C_{ii}}{\sum_{i=1}^{4}\sum_{j=1}^{4} C_{ij}} \quad (2)$$

where: $\sum_{i=1}^{4} C_{ii}$ is the total number of correct predictions for all classes (which is the sum of the elements on the main diagonal of the confusion matrix). $\sum_{i=1}^{4}\sum_{j=1}^{4} C_{ij}$ is the total number of data samples (which is the sum of all elements in the confusion matrix).

Precision

Precision measures the ratio of true positive predictions to all positive predictions. It is primarily used when we are interested in positive results and want to minimize false positive predictions (Maxwell et al., 2017). The precision for class i is calculated using the formula:

$$\text{Precision}_i = \frac{C_{ii}}{C_{ii} + \sum_{j \neq i} C_{ji}} \quad (3)$$

where: The numerator C_{ii} represents the total number of predictions for class i (both correct and incorrect). The denominator is the sum of C_{ii} and all values C_{ji}, which accounts for false positive predictions from other classes incorrectly predicted as class i.

Recall

Recall measures the ratio of actual positive samples that are correctly predicted. It is crucial when we want to minimize cases of missed detections (False Negatives) (Maxwell et al., 2017). The recall for class iii is calculated using the formula:

$$Recall_i = \frac{C_{ii}}{C_{ii} + \sum_{j \neq i} C_{ij}} \quad (4)$$

where: The numerator C_{ii} represents the number of correct predictions for class i. The denominator is the sum of C_{ii} and all values C_{ij}, which accounts for false negative predictions from other classes incorrectly predicted as another class.

F1-Score

F1-score is the harmonic mean between precision and recall, helping to balance the two measures. The F1-score is particularly useful in cases of imbalanced data (Draszawka and Szymański, 2023). The formula for calculating the F1-score for class i is:

$$F1 - score_i = 2\ x\ \frac{Precision_i\ x\ Recall_i}{Precision_i + Recall_i} \quad (5)$$

Area Under Curve (AUC)

AUC is a common metric for evaluating the performance of classification models, typically used for binary classification tasks. For multi-class classification problems, AUC is extended by calculating the AUC for each class and then aggregating these values (Wu and Zhou, 2017). In this context, the multi-class classification problem is transformed into several binary classification problems. Specifically, for each class, you compare that class against all other classes combined into a single class (Wu and Zhou, 2017). The AUC for each class is then calculated similarly to the binary case. The closer the AUC value is to 1, the more accurate the model.

Steps to calculate AUC for each class:

- Select a class *i*, then label this class as positive (Positive) and the remaining classes as negative (Negative).

- Calculate the true positive rate (TPR) and false positive rate (FPR) for each class *i*.

The formula for calculating AUC for each class is as follows:

$$AUC_i = \sum_{k=1}^{n-1} \frac{(TPR_{k+1} + TPR_k)}{2} (FPR_{k+1} - FPR_k) \quad (6)$$

where: TPR is the true positive rate (recall); FPR is the false positive rate. nnn is the total number of samples in class *i*.

The mean AUC value across classes is calculated by summing the AUCs for each class and dividing by the number of classes.

Kappa

Kappa measures the accuracy of the model while accounting for random factors. It assesses the agreement between the model's predictions and the actual labels, adjusting for any random outcomes that may occur (de la Torre, Puig and Valls, 2018). The formula for Kappa is:

$$Kappa = \frac{p_0 - p_e}{1 - p_e} \quad (7)$$

Where p_0 is the proportion of correct predictions made by the model, and p_e is the expected proportion of correct predictions due to chance, calculated by taking the product of the total number of correct predictions and the total number of actual predictions for each class.

Root Mean Square Error (RMSE)

RMSE measures the deviation between predicted and actual values, which is commonly used in regression problems. It represents the model's error level, with a smaller RMSE indicating better model performance (Wei and James, 2013). The formula for RMSE is:

$$RMSE = \sqrt{\frac{1}{n}\sum_{i=1}^{n}(y_i - \hat{y}_i)^2} \quad (8)$$

where y_i is the actual value of the *i*-th sample, $\hat{y}_i$ is the predicted value of the *i*-th sample, and *n* is the total number of data samples.

3.2. Data used

3.2.1. High-solution UAV images

The primary database in this study consists of two photogrammetry image scenes (Fig. 5), captured at two different time points (pre-scene: captured on January 31, 2023 (Fig. 5a) and post-scene: captured on October 20, 2023 (Fig. 5b)). The data for pre-scene was processed using images taken from a Mavic 3 drone (Fig. 6a) (Chenyan et al., 2024). Post-scene was processed using images from a Wingtra One GEN II drone (Fig. 6b) (Grubesic, Nelson, and Wei, 2024). The specifications of the two drones are presented in Table 2. Both scenes were processed to achieve an ordinary spatial resolution of 0.1266 m/pixel, with each image comprising three RGB spectral bands.

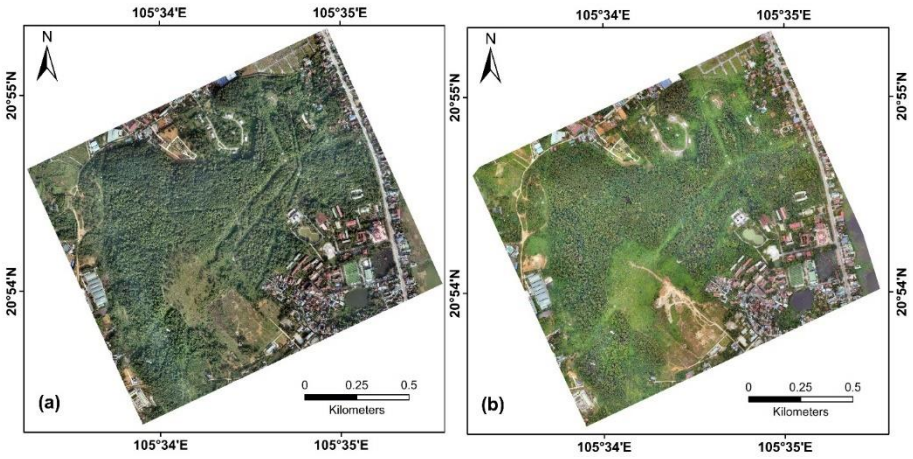

Figure 5. The photogrammetry scenes in the study area: (a) pre-scene, (b) post-scene